Active controlled and tunable coacervation using side-chain functional α-helical homopolypeptides

Wendell A. Scott[a], Eric G. Gharakhanian[a], Alexandra G. Bell[a], Declan Evans[a], Ehab Barun[a], K. N. Houk[a], Timothy J. Deming[a,b,c*]

[a] Department of Chemistry and Biochemistry, University of California, Los Angeles, CA 90095, USA

[b] Department of Bioengineering, University of California, Los Angeles, CA 90095, USA

[c] California NanoSystems Institute, University of California, Los Angeles, CA 90095, USA

Abstract

We report the development of new side-chain amino-acid functionalized α-helical homopolypeptides that reversibly form coacervate phases in aqueous media. The designed multifunctional nature of the side-chains was found to provide means to actively control coacervation via mild, biomimetic redox chemistry, as well as allow response to physiologically relevant environmental changes in pH, temperature and counterions. These homopolypeptides were found to possess properties that mimic many of those observed in natural coacervate forming intrinsically disordered proteins. Despite ordered α-helical conformations that are thought to disfavor coacervation, molecular dynamics simulations of a polypeptide model revealed a high degree of side-chain conformational disorder and hydration around the ordered backbone, which may explain the ability of these polypeptides to form coacervates. Overall, the modular design, uniform nature, and ordered chain conformations of these polypeptides were found to provide a well-defined platform for deconvolution of molecular elements that influence biopolymer coacervation and tuning of coacervate properties for downstream applications.

Introduction

Much of the recent interest in biomimetic coacervates stems from the discovery of membraneless organelle (MLO) domains that form within cells via liquid-liquid phase separation.[1,2] These domains are typically enriched in intrinsically disordered proteins and are involved in many transient biological processes,[1,2] which are often under active enzymatic control via post-translational protein modifications.[3-6] With the goal of better understanding MLOs and mimicking their ability to concentrate molecules and catalyze reactions, significant advances have been made in development of a variety of coacervate models.[7,8] However, due to compositional complexity or limited functionality there remains a need for well-defined and tunable biomimetic models capable of replicating the many features found in MLOs, including responsiveness to multiple stimuli and active control of coacervation.[3-8] Here, we report the design and evaluation a new class of compositionally uniform, α-helical homopolypeptides capable of coacervation in aqueous media. Despite ordered chain conformations that are thought to disfavor coacervation,[9] the incorporation of side-chain amino acid functionality imparts these homopolypeptides with numerous tunable, modular components that enable coacervation in response to biologically relevant environmental stimuli as well as through reversible biomimetic chemical modification. The ability to systematically adjust side-chain components in these polypeptides provides a means to elucidate molecular features necessary for coacervation and to fine-tune properties for downstream uses.

Numerous peptide based coacervate-forming model systems have been developed,[7,8] including those based on recombinant proteins,[10-14] peptide sequences,[15-20] and synthetic polypeptides.[21-28] Model coacervates developed using engineered proteins contain specific sequences that can provide selective binding to other biomolecules and can also respond to changes in pH and ionic strength within physiological ranges.[11] Some of these systems can form coacervates in response to temperature changes,[10,12,14] and others have been engineered to enable active control by redox chemistry or enzymatic cleavage.[13] A challenge with protein based coacervate models is the difficulty in deconvolution of complex sequences such that design rules for tuning coacervation properties are not fully understood.[1-8] Sequence-specific peptides provide an alternative to proteins, where their smaller size and often simpler

sequence can allow for improved understanding of structure-property relationships. Peptide containing coacervates have been reported that can be actively controlled by enzymatic phosphorylation/dephosphorylation of serine residues,[16] or by reduction/oxidation of disulfide linkages.[20] These systems mimic features found in protein coacervates, and in a minimal dipeptide system have been used to understand how substitution of amino acids, such as leucine, phenylalanine, and tryptophan, affects coacervation.[20] However, more complex peptide sequences suffer the same challenge as proteins in that molecular design rules are not fully understood.[1-8]

Synthetic polypeptide based coacervates consist mainly of highly charged, simple sequences (e.g. homopolymers of lysine or glutamic acid),[21-28] which offer few opportunities to tune or actively modify coacervate properties at the molecular level. These systems possess limited response to pH, temperature, and ionic strength within physiological ranges.[21-28] One type of model system relies primarily on polyelectrolyte complexation between two oppositely charged polypeptides, i.e. complex coacervation.[9,22-24,28] In examples of this model, it has been reported that at least one macromolecular component must possess a disordered conformation to prevent precipitation of solids.[28] Another well-studied model system is based on coacervation of cationic homopolypeptides (e.g. poly(L-lysine)) with anionic nucleotides and polynucleotides.[21,25-27] Noteworthy achievements in examples of this model include the demonstration of active control of coacervation by enzymatic interconversion of ATP and ADP nucleotides in mixtures with poly(L-lysine),[25] as well as formation of temperature dependent liquid crystalline coacervate phases in mixtures of poly(L-lysine) with short dsDNA containing complimentary sticky ends that can self-assemble in the coacervate phase.[26] Contrary to the active control observed in protein coacervates that results from enzymatic post-translational modification of amino acid residues,[1-6] the responsive behavior in these examples does not arise from the polypeptide components, which function primarily as disordered polycations.

To bridge the gap between polypeptide and peptide/protein coacervate models, we sought to develop synthetic polypeptides that could replicate most of the features found in coacervate forming proteins, such as the ability to respond to changes in pH, ionic strength, and temperature within physiologically relevant ranges.[1-8] The ability to actively control coacervation via reversible polypeptide

modification, mimicking post-translational modifications in protein coacervates,[1-6] was also deemed important. In addition, we desired a modular design with many readily adjustable functional elements to allow deconvolution of molecular requirements for coacervation and for fine tuning of coacervate properties for downstream uses. To decouple the presence of multiple functional groups from concomitant peptide sequence complexity,[10-19] we avoided copolypeptide designs and instead pursued a new concept centered on homopolypeptide chains that contain multiple, precisely located functional elements in each side-chain group.

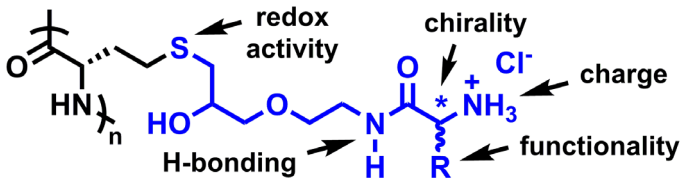

Scheme 1. Structure showing proposed tunable features of amino acid functionalized poly(S-alkyl-L-homocysteine)s

Specifically, our design incorporates amino acid components into the side-chains of a poly(S-alkyl-L-homocysteine) scaffold (Scheme 1). This homopolypeptide backbone was chosen because it favors an α-helical conformation in water that can be readily and reversibly converted to a disordered conformation upon mild oxidation to the sulfoxide derivative.[29,30] The incorporation of amino acids as side-chain functionality was envisioned to enhance the polypeptide side-chains with many adjustable molecular features commonly found in proteins, such as H-bonding from amide groups, charges from carboxylate or ammonium groups, chirality, as well as hydrophobicity or other functionality from the amino acid "R" groups (Scheme 1). Through designed combinations of charge, hydrophobicity, hydrophilicity, and side-chain flexibility, we sought to develop a homopolypeptide based coacervate system with tunable properties that can respond to multiple biologically relevant stimuli and chemical modifications.

Results and Discussion

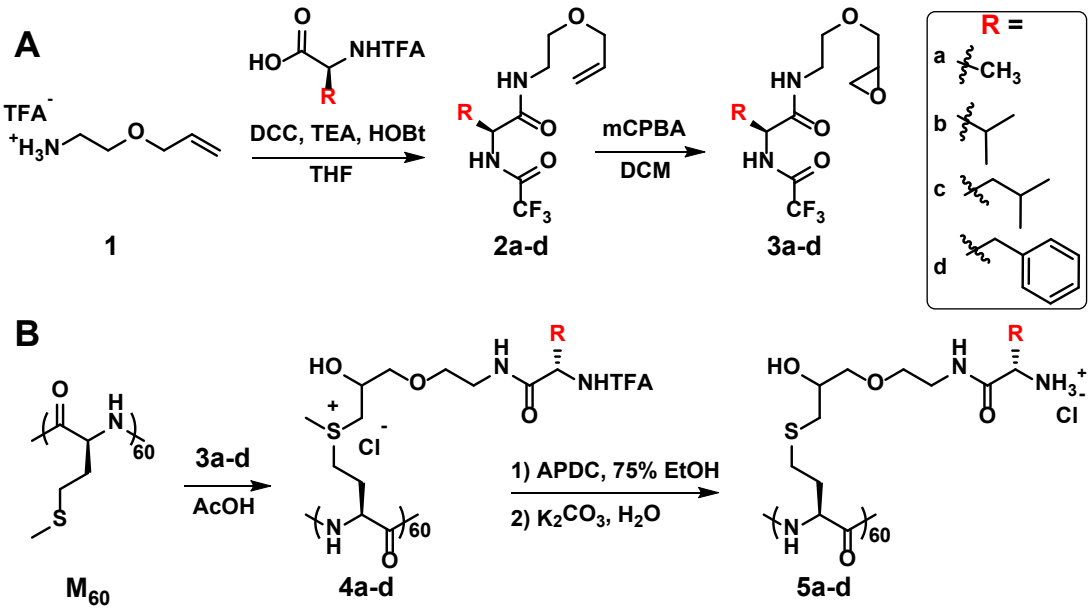

Scheme 2. Synthesis of intermediates and homopolypeptide samples **5a**-**5d**. DCC = dicyclohexylcarbodiimide; TEA = trietrimethylamine, HOBt = 1-hydroxybenzotriazole; THF = tetrahydrofuran; mCPBA = meta-chloroperbenzoic acid; DCM = dichloromethane; AcOH = acetic acid; APDC = ammonium pyrrolidinedithiocarbamate; EtOH = ethanol.

For our initial design, we prepared the series of amino acid functionalized poly(S-alkyl-L-homocysteine) samples **5a**-**5d** shown in Scheme 2. In these samples, amino acids were connected to the polypeptide backbone via their carboxylic acid functionality such that the side-chains contain terminal primary amine groups, allowing for formation of cationic polypeptides. Although analogous anionic, carboxylate terminated polypeptides could be prepared by reversal of the amino acid linkage,[31] we chose cationic polypeptides to better mimic the numerous protein coacervates that bind nucleic acids and polynucleic acids.[32] Samples **5a**-**5d** were synthesized in a modular approach using readily prepared epoxide derivatives of the amino acids, **3a**-**3d** (see SI, Table S1), where the amino acids L-alanine (Ala), L-valine (Val), L-leucine (Leu), and L-phenylalanine (Phe) were chosen to present a range of hydrophobicity. Epoxides **3a**-**3d** were then each incorporated into a common poly(L-methionine)$_{60}$, **M$_{60}$**, precursor using our recently developed methodology for efficient conversion of methionine residues to functionalized S-alkyl homocysteine residues (overall isolated yields for polypeptide modification *ca*. 73-

83%, Scheme 2, see Table S1).[31,33] ^{1}H and ^{13}C NMR analysis of **5a**-**5d** showed that methionine residues were fully converted to the corresponding functionalized residues for each sample.

Samples **5a**-**5d** were purified by dialysis against aqueous HCl (3 mM) followed by deionized water to give the polypeptides as white powders after lyophilization. For samples **5c** and **5d**, dissolution in minimal trifluoroacetic acid before dialysis was found to enhance dissolution. The resulting protonated polypeptides **5a**-**5d** with Cl^- counterions were all found to be soluble in deionized water at 20 °C. Since α-amine groups on peptides are known to have substantially lower pK_a values compared to aliphatic amines,[34] we examined the degree of protonation for **5a**-**5d** in 20 mM aqueous NaCl as a function of pH. Measurement of Zeta potential for solutions of **5a**-**5d** as a function of pH revealed transitions from positive to moderately negative values between pH 6 and 9, indicative of a change from protonated to non-protonated α-amine groups over this pH range (Figure 1).[35] This transition correlates well with the expected pK_a range of α-amino amide groups (*ca*. 7 to 8),[34] and was corroborated by analysis of other control samples that included non-ionic poly(L-methionine sulfoxide)$_{60}$, pH invariant cationic poly(S-methyl-L-methionine sulfonium chloride)$_{60}$, and poly(L-lysine·HCl)$_{60}$ that undergoes a protonated to non-protonated transition at a much higher pH (pK_a *ca*. 9.5 to 10) (Figure 1).[35,36] These results show that **5a**-**5d** side-chains can undergo protonation and deprotonation within a physiological range of pH, which is advantageous for biologically relevant adjustment of physical properties (*vide infra*) and contrasts other amine containing polymers used in coacervation models that have much higher pK_a values (e.g. poly(L-lysine).

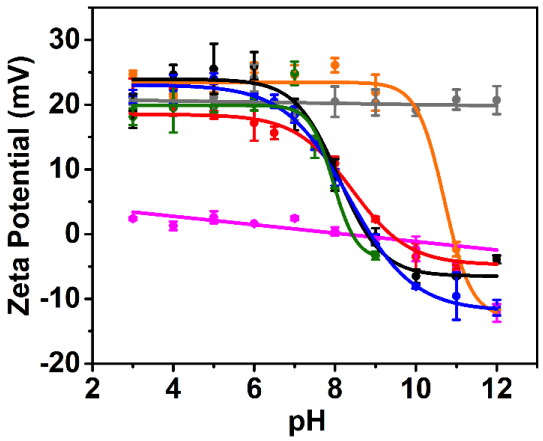

Figure 1. Zeta Potential measurements of polypeptide samples as a function of solution pH. Measurements of polypeptides **5a**-**5d** and reference polypeptides were performed at 5.0 mg/mL in 20 mM NaCl at 20 °C. **5a** = black; **5b** = red; **5c** = blue; **5d** = green; poly(L-lysine·HCl)$_{60}$ = orange; poly(S-methyl-L-methionine sulfonium chloride)$_{60}$ = grey; poly(L-methionine sulfoxide)$_{60}$ = magenta. Data was not recorded above pH 9 for sample **5d** due to phase separation. Error bars represent standard deviations of triplicate measurements.

To determine how the degree of protonation of **5a**-**5d** influences their chain conformations in aqueous media, each polypeptide was analyzed using circular dichroism (CD) spectroscopy over a range of pH in aqueous phosphate buffer (Figure 2). At pH 5.5, where all chains were highly charged, CD spectra revealed that **5a**-**5d** predominantly adopt α-helical conformations (*ca*. 70% α-helical content, see Table S2).[37] The high α-helical content of these charged polypeptides is not entirely unexpected since we have reported that other poly(S-alkyl-L-homocysteines) adopt α-helical conformations,[29,30,38] and it has been shown that placing charged groups sufficiently distant from the polypeptide backbone minimizes their perturbation of α-helical conformations in water.[39] As solution pH was increased, the α-helical contents of **5a**-**5c** were all found to increase to *ca*. 85-90% as side-chain amine groups were deprotonated and chains were neutralized. Sample **5d** was not soluble in phosphate buffer above pH 5.5, likely due to the hydrophobicity of the Phe side-chain group (*vide infra*). The samples with less hydrophobic side-chains, especially **5a** and **5b**, were soluble and α-helical up to pH 9.0, where the chains are expected to contain few charges. Overall, these CD data show that **5a**-**5d** predominantly adopt α-helical conformations, which are stable over a biologically relevant range of pH in water.

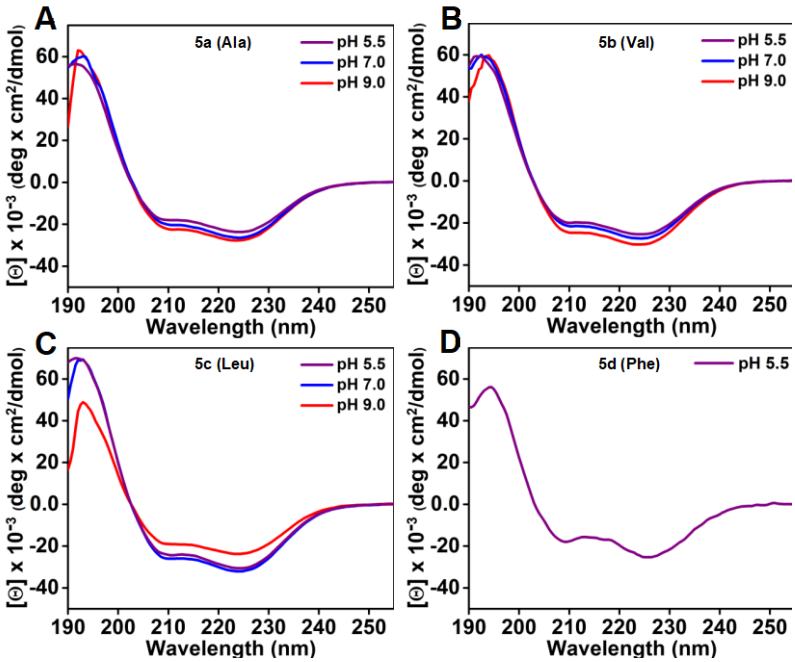

Figure 2. Circular dichroism spectra of polypeptide samples **5a-5d** at different solution pH. A) **5a**; B) **5b**; C) **5c**; D) **5d**. Samples **5a-5c** were prepared at 0.5 mg/mL in pH 5.5, 7.0 or 9.0 phosphate buffer (100 mM) at 20 °C. Sample **5d** was prepared at 0.1 mg/mL in pH 5.5 phosphate buffer (20 mM) at 20 °C. Sample **5d** is not soluble in phosphate buffer at pH 7.0 or 9.0.

We next sought to evaluate the aqueous phase behavior of **5a**-**5d** as functions of varying pH, temperature and counterions. For the initial study, dilute aqueous solutions of **5a**-**5d** (3.0 mg/mL) were prepared in 150 mM phosphate buffer saline (PBS) buffer at pH values ranging from 6.5 to 8.0, which were chosen to include varying degrees of polypeptide protonation. These solutions were heated at a controlled rate up to 90 °C (see SI), and optical transmittance at 500 nm was measured as a function of temperature. The least hydrophobic sample **5a** was found to remain soluble up to 90 °C (see Table S3), while the more hydrophobic **5b**-**5d** were found to phase separate in a pH and temperature dependent manner (Figure 3a-c, see Table S3). Reversible cloud points were observed for **5b**-**5d** upon increase in temperature, indicative of lower critical solution temperature (LCST) induced phase separation,[40] with cloud point temperatures (T_{cp}) that decreased with increasing hydrophobicity of side-chain amino acids in the order Val < Leu < Phe.[41] Cloud point temperatures for **5b**-**5d** also decreased as pH was increased,

which is consistent with other partially charged thermoresponsive polymers where T_{cp} decreases substantially as charge is removed from the polymer chains.[42] The results of this study show that **5b**-**5d** in 150 mM PBS buffer can undergo phase separation from aqueous solution at physiologically relevant temperatures, ionic strength and solution pH, where T_{cp} can be predictably tuned by variation of polypeptide side-chain amino acid hydrophobicity.

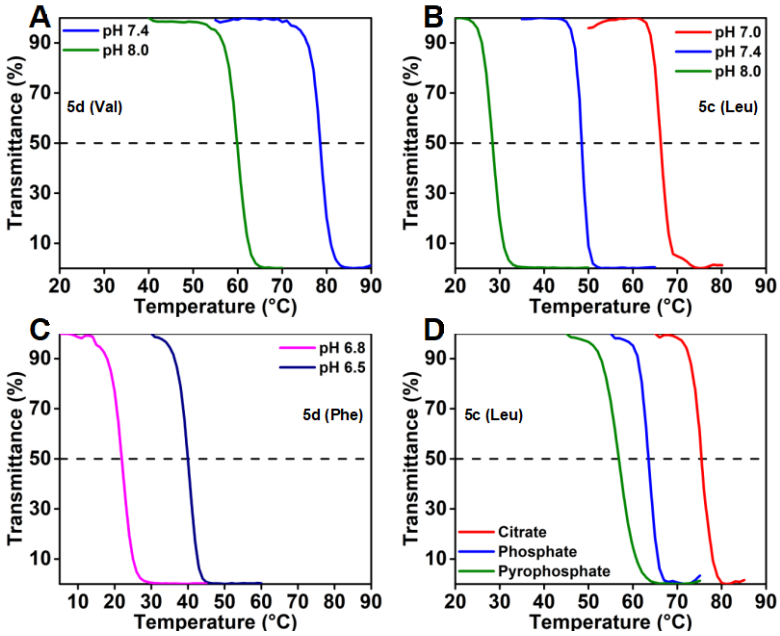

Figure 3. Temperature dependent coacervate formation in solutions of polypeptides **5b, 5c** and **5d** as functions of pH and counterions. Panels show optical transmittance at 500 nm for 3.0 mg/mL solutions of polypeptides in 150 mM PBS buffer measured at different pH over a range of temperature. A) **5b**; B) **5c**; C) **5d**. D) Optical transmittance at 500 nm for 3.0 mg/mL solutions of **5c** in 150 mM NaCl measured in the presence of sodium salts of different counterions (12 mM) at pH 7.0 over a range of temperature.

Having observed that the substitution of phosphate for chloride decreases the solubility of **5d** in water (Figure 2), we further investigated the effects of counterion valency on aqueous phase separation of **5a**-**5d**. Aqueous samples of **5a**-**5d** (3.0 mg/mL) were prepared in 150 mM NaCl at pH 7 and then mixed with sodium salts of anionic counterions with different valency (12 mM final concentration, Table 1). Note that the most hydrophobic sample, **5d**, did not dissolve in water with any counterion at pH 7 and 20 °C. In general, as anion valency was increased, all samples became less soluble in water. This result is

explained by increased stability of ion complexes between the cationic polypeptides and anions with higher valency. Even the more hydrophilic samples, **5a** and **5b**, were found to undergo phase separation in the presence of pyrophosphate or tripolyphosphate anions at 20 °C. Intermediate hydrophobicity sample **5c** was the most interesting because its temperature dependent water solubility was found to vary with anion valency. While high valent tripolyphosphate caused **5c** to phase separate at 20 °C, other anions were found to give cloud point temperatures that in general varied inversely with anion valency (Figure 3d, Table 1). Hence, in addition to pH and side-chain amino acid hydrophobicity, counterions provide another means to fine tune phase transition temperature of these homopolypeptides.

Table 1. Coacervate transition temperatures for solutions of polypeptides **5a**-**5d** containing different counterions. Cloud point temperatures (T_{cp}) were measured for individual 3.0 mg/mL solutions of **5a**-**5d** in the presence of different counterions (12 mM) in 150 mM NaCl at pH 7.0. sol = polypeptide was soluble up to 90 °C. -- = polypeptide formed a coacervate at 20 °C. ppt = polypeptide formed a solid precipitate, not a coacervate, at 20 °C.

Counterion	**Ion valency at pH 7.0**	**Ionizable Sites**	**T_{cp} of 5a (°C)**	**T_{cp} of 5b (°C)**	**T_{cp} of 5c (°C)**	**T_{cp} of 5d (°C)**
Chloride	-1.0	1	sol	sol	sol	--
Sulfate	-2.0	2	sol	sol	sol	--
Phosphate	-1.4	3	sol	sol	64	--
Citrate	-3.0	3	sol	sol	75	--
Pyrophosphate	-2.7	4	ppt	sol	57	--
Tripolyphosphate	-4.0	5	ppt	--	--	--

To investigate the nature of phase separation in **5a**-**5d** samples described above, the suspensions formed in the presence of tripolyphosphate anions at pH 7.0 were allowed to settle onto glass slides and were examined using differential interference contrast (DIC) optical microscopy (Figure 4). Images of the complex formed with least hydrophobic **5a** showed irregular edges and clusters

consistent with formation of a solid precipitate. However, images of tripolyphosphate complexes with **5b**-**5d** all showed smooth outlines and coalescing droplets consistent with formation of liquid coacervate phases.[7,8] For additional confirmation of coacervate formation, centrifugation of the **5c**-tripolyphosphate suspension resulted in the formation of two separate liquid layers (see Figure S1). Examination of the phase separated complexes of **5d** with different counterions, including chloride (Table 1), also showed coacervate formation in all cases (see Figure S1). In addition to coacervation with simple counterions, **5c** was also able to form a complex coacervate with a model RNA sequence, polyadenylic acid, at 20 °C (see Figure S2), which is advantageous for downstream development of simplified models of protein-RNA coacervates.[7,8]

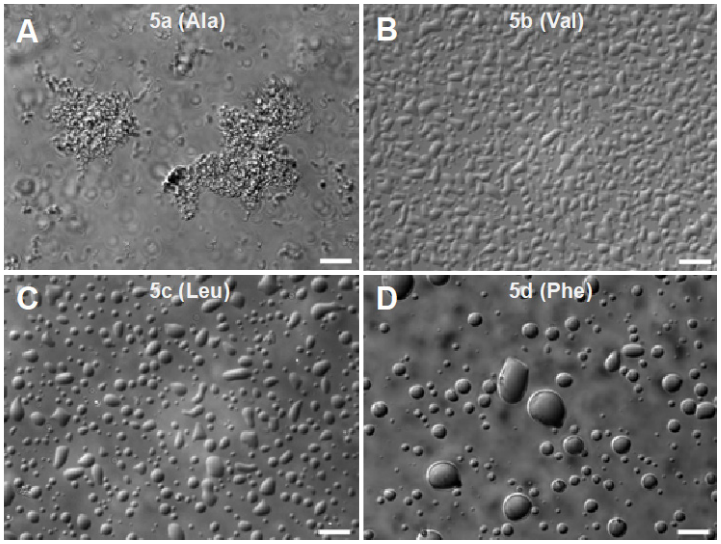

Figure 4. Optical micrographs of polypeptide mixtures with sodium tripolyphosphate. Solutions of polypeptides **5a**-**5d** at 3.0 mg/mL in 150 mM NaCl at 20 °C and pH 7.0 were mixed with sodium tripolyphosphate (12 mM final concentration) and the resulting turbid suspensions were allowed to settle onto glass slides. A) **5a**; B) **5b**; C) **5c**; D) **5d**. Scale bars = 20 μm.

Although the images described above show **5b**-**5d** form coacervates at 20 °C, we also imaged the phase separation of **5c** in PBS buffer at pH 8 and 45 °C (Figure 3) to see if coacervation occurs at elevated temperature as well. DIC microscopy of this sample confirmed the formation of coacervate droplets (see Figure S2). Coacervate formation in this sample was also found to be highly reversible with

no signs of irreversible polypeptide aggregation. Multiple heating and cooling cycles were applied to the mixture of **5c** in PBS buffer at pH 8 and monitored by optical transmittance, where coacervation and complete dissolution were observed with each thermal cycle (Figure 5a). Finally, as an initial study of salt stability, complexes of **5c** with tripolyphosphate were prepared in aqueous solutions containing 0 to 500 mM NaCl. As ionic strength was increased up to 250 mM NaCl, the fraction of **5c** that partitioned into the coacervate phase decreased, and no phase separation occurred at higher salt concentrations (Figure 5b). At 150mM NaCl, the coacervate phase was found via thermogravimetric analysis to contain *ca*. 50% water by weight (see Figure S3). These results are consistent with trends observed for many coacervate systems,[7,8] and show that this **5c** coacervate is stable at physiological ionic strength.

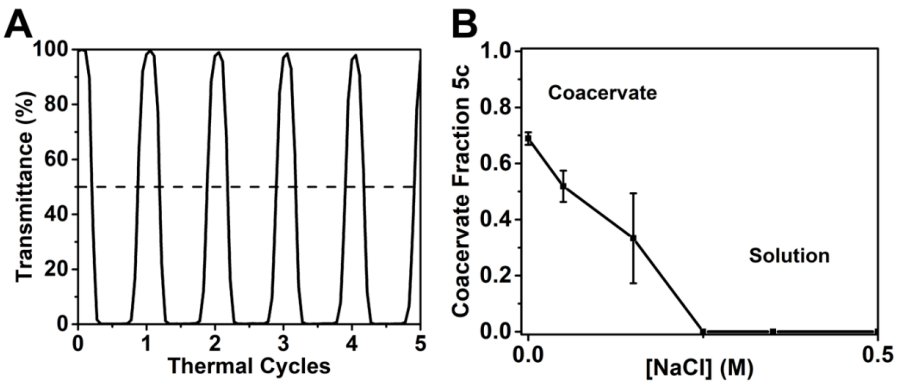

Figure 5. A) Reversibility of temperature dependent coacervate formation for polypeptide **5c** in PBS buffer as determined by optical transmittance at 500 nm. Sample was prepared at 3.0 mg/mL in 150 mM PBS buffer at pH 8.0 and subjected to repeated thermal cycling between 17 and 44 °C. Sample was heated and cooled at the rate of 3 °C/min. B) Coacervate formation of **5c** mixed with sodium tripolyphosphate as a function of sodium chloride concentration. Coacervate Fraction = (mass of polypeptide in coacervate phase)/(total mass of polypeptide). Samples were prepared by mixing **5c** (3.0 mg/mL) in different concentrations of NaCl at 20 °C and pH 7.0 with sodium tripolyphosphate (12 mM final concentration). Error bars represent standard deviations of triplicate measurements.

A remarkable feature of the **5b**-**5d** coacervates is the stable α-helical conformation of these homopolypeptides. Most coacervate forming proteins are highly disordered,[7,8,10-14] and all other synthetic

polypeptide based coacervates rely on conformational disorder in at least one of the macromolecular components.[9,21-28] The current dogma of coacervate formation using homopolypeptides demands a conformationally disordered component to prevent solid precipitate formation.[28] We showed above that **5b**-**5d** possess stable α-helical conformations in dilute aqueous solution over a range of pH (Figure 2). To confirm that the polypeptides retain their α-helical conformations in coacervates, we isolated the polymer-rich coacervate phase from a mixture of **5c** and tripolyphosphate in 150 mM NaCl at pH 7.0. The CD spectrum collected from a thin film of this coacervate showed the presence of the characteristic double minima consistent with a predominantly α-helical conformation (see Figure S4).[37] To better understand the ability of these α-helical polypeptides to form coacervates and not precipitates, we also performed molecular dynamics (MD) simulations on a 15-mer model of **5c**. These simulations show that the backbone atoms are conformationally stable with root-mean-square deviation (RMSD) values of around 2 Å (Figure 6). Alpha carbons overlay well, and the α-helix is clearly visible throughout the simulations. The side-chains, in contrast, are highly disordered with RMSD values of 8-12 Å and adopt a wide range of conformations. This high degree of disorder in the side-chains accounts for most of the total RMSD of the polypeptide chains and may explain the ability of **5b**-**5d** to form coacervates despite their highly structured backbones (see Figure S5). In addition, hydroxyl and amide groups in the side-chains and backbone regularly hydrogen bond with water molecules, suggesting these polymers do not completely exclude water at 300K (see Figure S6). The retention of water within the side-chains due to hydrogen bonding may explain the ability of these polymers to form coacervates instead of precipitates.

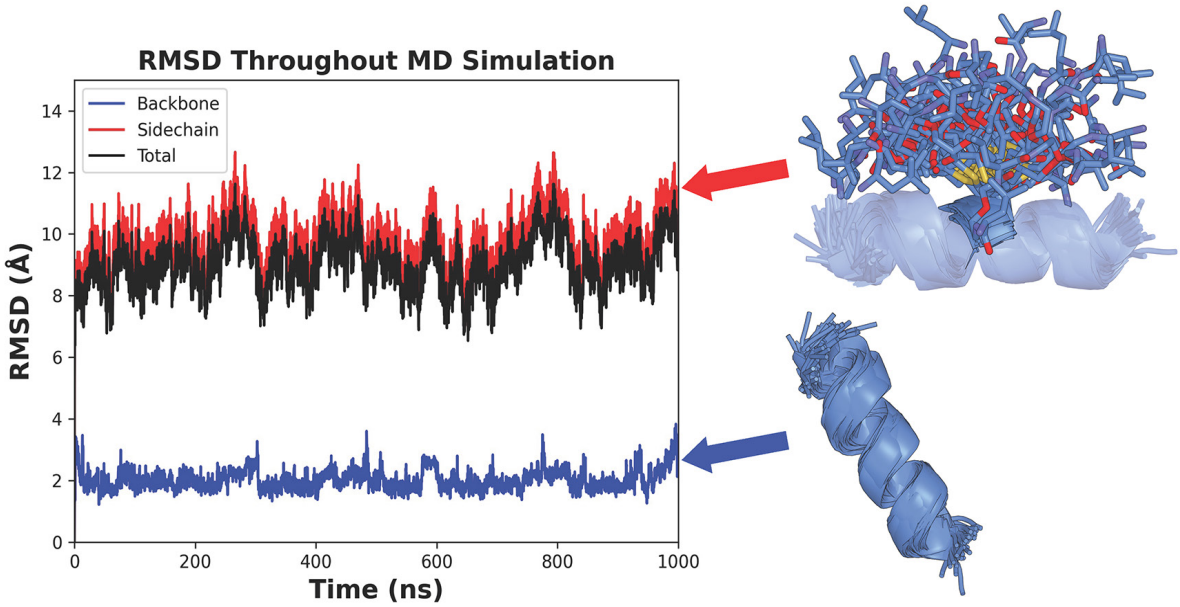

Figure 6. Calculated RMSD of backbone atoms (blue), side-chain atoms (red) and all atoms (black) for a 1000 ns MD simulation of a 15-mer of **5c**. Backbone atoms have very low RMSD, and overlaying alpha carbons shows that the α-helix is clearly visible (lower right). Side-chain atoms have very high RMSD, and overlaying different conformers of a single residue (number 8) shows that the side-chains adopt a high degree of conformational flexibility (upper right).

An additional feature of poly(S-alkyl-L-homocysteine)s is that their stable α-helical conformations in water can be disrupted to disordered conformations upon oxidation of side-chain thioether groups to sulfoxides.[29,30] Such oxidation can occur under mild conditions, with the intracellular oxidation of methionine residues in proteins being a well-known example.[43] It has also been established that ubiquitous reductase enzymes can readily reduce intracellular methionine sulfoxide residues in proteins,[44-46] and we have shown this can also be accomplished with synthetic poly(L-methionine sulfoxide) substrates *in vitro*.[29] As such, reversible oxidation of side-chain thioether groups in **5a**-**5d** was investigated as a means to actively control their coacervation, akin to how post-translational modifications are used to control protein coacervation within cells.[3-6] A sample of **5c** was oxidized to give the corresponding sulfoxide derivative **6c** using *tert*-butyl hydroperoxide in water (Scheme 3).[35] Polypeptide

6c was soluble in deionized water, and CD spectroscopy analysis showed that it possessed a highly disordered chain conformation as compared to **5c** (Figure 7a). This conformational switch is consistent with results of our prior studies on non-ionic, water soluble poly(S-alkyl-L-homocysteine) derivatives,[30,38] and is likely due to the high degree of solvation of sulfoxide groups by water molecules that leads to disruption of backbone H-bonding.[47]

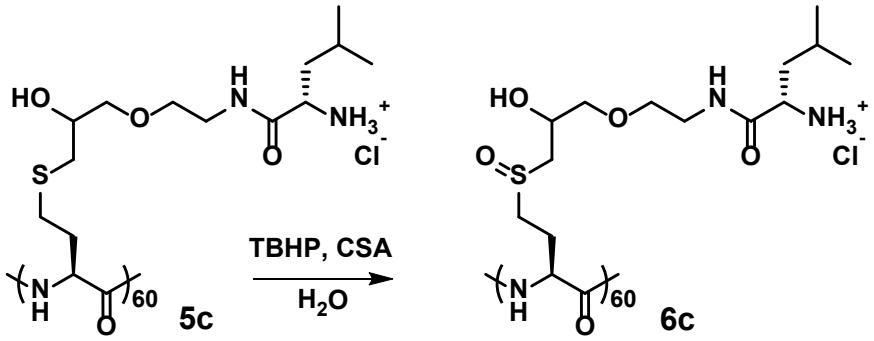

Scheme 3. Synthesis of sulfoxide derivative **6c** from **5c**. TBHP = *tert*-butyl hydroperoxide. CSA = camphorsulfonic acid.

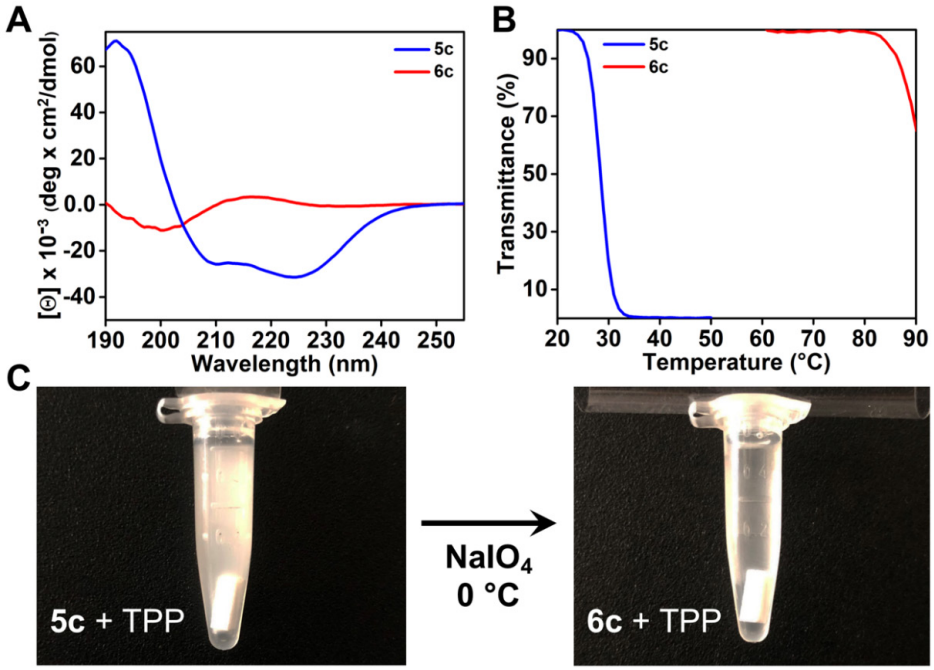

Figure 7. A) Circular dichroism spectra of **5c** and oxidized polypeptide **6c** both at 0.5 mg/mL in DI water and 20 °C. B) Temperature dependent coacervate formation of polypeptides **5c** and **6c** in 150 mM PBS buffer as determined by optical transmittance at 500 nm. Each sample was prepared at 3.0 mg/mL

polypeptide and pH 8.0. C) Images of coacervate phase of **5c** mixed with sodium tripolyphosphate before (left) and after oxidation to **6c** using sodium periodate (0.5 M, 1.05 eq over 2 additions) at 0 °C (right). Initial sample was prepared by mixing **5c** (3.0 mg/mL) in 150 mM NaCl at 20 °C and pH 7.0 with sodium tripolyphosphate (12 mM final concentration).

The increased hydrophilicity of **6c** relative to **5c** had a striking effect on its temperature dependent phase separation. When **6c** was dissolved in 150 mM PBS buffer at pH 8, the polypeptide remained soluble as the sample was heated and only started to phase separate above 80 °C. This contrasts drastically with **5c**, which possesses a cloud point temperature of 28 °C under the same conditions (Figure 7b). Hence, it would be expected that coacervation could be actively controlled by interconversion of **5c** and **6c**. Such active control was demonstrated by addition of one equivalent of $NaIO_4$ oxidant at 0 °C to a coacervate suspension of **5c** mixed with tripolyphosphate (Figure 7c). Within 10 minutes, the coacervate droplets were observed to completely dissolve as **5c** was oxidized to **6c**. ^{1}H NMR spectroscopy of the product after 2 hours showed *ca*. 73% oxidation of **5c** residues (see SI), indicating that complete oxidation is not required to dissolve the coacervate phase. Also, ^{1}H NMR analysis confirmed exclusive formation of the sulfoxide **6c**, without any formation of sulfone byproducts (see Figure S7). Reduction of **6c** back to **5c** was also accomplished using sodium thioglycolate (see Scheme S1), which confirmed the reversibility of this process. In related work, Spruijt has developed an elegant small molecule system based on cleavage of disulfide linkages between peptides that also displays redox reversible coacervation.[20] As far as we are aware, the **5c**/**6c** system reported here is the first actively controlled polypeptide coacervate that utilizes non-destructive, biologically relevant chemical modification akin to post-translational modification in proteins.

Conclusions

We have designed new, side-chain amino-acid functionalized homopolypeptides that reversibly form coacervate phases in aqueous media. The multifunctional nature of the side-chains provides means to actively control coacervation via mild, biomimetic redox chemistry, as well as enables the ability to respond to physiologically relevant environmental changes in pH, temperature and counterions. The

modular design, uniform nature, and ordered chain conformation of these homopolypeptides provides a well-defined platform that can be used to create additional new polypeptides for tuning coacervate properties and deconvolute molecular elements that affect coacervation, as exemplified here by variation of amino acid hydrophobicity. These homopolypeptides were found to possess properties that mimic many of those observed in natural coacervate forming proteins, including IDPs.[1-6] As such, this polypeptide platform may be amenable for use as mimics of IDPs, as tunable models to help understand their properties, as stimuli controlled microreactors, or in downstream uses including therapeutic delivery and protein separation.

Associated Content

Supporting Information

The Supporting Information is available free of charge on the ACS Publications website at DOI: 10.1021/jacs.#######.

Experimental procedures, spectral data, additional images, CD spectra and computational data, and methods for all coacervate characterization (PDF).

Author Information

Corresponding Author

* demingt@seas.ucla.edu

ORCID

Timothy J. Deming: 0000-0002-0594-5025

Kendall N. Houk: 0000-0002-8387-5261

Notes

The authors declare no competing financial interest.

Acknowledgments.

All calculations were performed on the Hoffman2 cluster at the University of California, Los Angeles. This work was supported by NSF (MSN-1807362 to TJD), the UCLA Chemistry-Biology Interface training program, NIH, under grant No. T32GM008496 (to DE), and a Summer Undergraduate Research Fellowship from the UCLA Chemistry and Biochemistry Department (to AGB).

References:

1) Brangwynne, C. P. Soft active aggregates: mechanics, dynamics and self-assembly of liquid-like intracellular protein bodies. *Soft Matter* **2011**, *7*, 3052-3059.

2) Dzuricky, M.; Roberts, S.; Chilkoti, A. Convergence of artificial protein polymers and intrinsically disordered proteins. *Biochemistry* **2018**, *57*, 2405-2414.

3) Waite, J. H. Mussel adhesion – essential footwork. *J. Exp. Biol.* **2017**, *220*, 517-530.

4) Banani, S. F.; Lee, H. O.; Hyman, A. A.; Rosen, M. K. Biomolecular condensates: organizers of cellular biochemistry. *Nat. Rev. Mol. Cell. Biol*. **2017**, *18*, 285–298.

5) Kapelner, R. A.; Yeong, V.; Obermeyer, A. C. Molecular determinants of protein-based coacervates. *Curr. Opin. Coll. Int. Sci*. **2021**, *52*, 101407.

6) Yewdall, N. A.; André, A. A. M.; Lu, T.; Spruijt, E. Coacervates as models of membraneless organelles. *Curr. Opin. Coll. Int. Sci*. **2021**, *52*, 101416.

7) Roberts, S.; Dzuricky, M.; Chilkoti, A. Elastin-like polypeptides as models of intrinsically disordered proteins. *FEBS Lett.* **2015**, *589*, 2477-2486.

8) Abbas, M.; Lipiński, W. P.; Wang, J.; Spruijt, E. Peptide-based coacervates as biomimetic protocells. *Chem. Soc. Rev.* **2021**, 50, 3690-3705.

9) Perry, S. L.; Leon, L.; Hoffmann, K. Q.; Kade, M. L.; Priftis, D.; Black, K. A.; Wong, D.; Klein, R. A.; Piercel II, C. F.; Margossian, K. O.; Whitmer, J. K.; Qin, J.; de Pablo, J. J.; Tirrell, M. Chirality-selected phase behaviour in ionic polypeptide complexes. *Nat. Commun.* **2015**, *6*, 6052, DOI: 10.1038/ncomms7052.

10) Quiroz, F. G.; Chilkoti, A. Sequence heuristics to encode phase behaviour in intrinsically disordered protein polymers. *Nat. Mater.* **2015**, *14*, 1164–1171.

11) Wei, W.; Tan, Y.; Martinez Rodriguez, N. R.; Yu, J.; Israelachvili, J. N.; Waite, J. H. A mussel-derived one component adhesive coacervate. *Acta Biomater.* **2014**, *10*, 1663–1670.

12) Reed, E. H.; Hammer, D. A. Redox sensitive protein droplets from recombinant oleosin. *Soft Matter* **2018**,*14*, 6506-6513.

13) Schuster, B. S.; Reed, E. H.; Parthasarathy, R.; Jahnke, C. N.; Caldwell, R. M.; Bermudez, J. G.; Ramage, H.; Good, M. C.; Hammer, D. A. Controllable protein phase separation and modular recruitment to form responsive membraneless organelles. *Nat. Commun.* **2018**, *9*, 2985, DOI: 10.1038/s41467-018-05403-1

14) Dzuricky, M.; Rogers, B. A.; Shahid, A.; Cremer, P. S.; Chilkoti, A. De novo engineering of intracellular condensates using artificial disordered proteins. *Nat. Chem.* **2020**, *12*, 814–825.

15) Semenov, S. N.; Wong, A. S. Y.; van der Made, R. M.; Postma, S. G. J.; Groen, J.; van Roekel, H. W. H.; de Greef, T. F. A.; Huck, W. T. S. Rational design of functional and tunable oscillating enzymatic networks. *Nat. Chem.* **2015**, *7*, 160–165.

16) Aumiller, W. M.; Keating, C. D. Phosphorylation-mediated RNA/peptide complex coacervation as a model for intracellular liquid organelles. *Nat. Chem.* **2016**, *8*, 129–137.

17) Kaminker, I.; Wei, W.; Schrader, A. M.; Talmon, Y.; Valentine M. T.; Isrealachvili, J. N.; Waite, J. H.; Han, S. Simple peptide coacervates adapted for rapid pressure-sensitive wet adhesion. *Soft Matter,* **2017**, *13*, 9122-9131.

18) Chang, L. W.; Lytle, T. K.; Radhakrishna, M.; Madinya, J. J.; Vélez, J.; Sing, C. E.; Perry, S. L. Sequence and entropy-based control of complex coacervates. *Nat. Commun.* **2017**, *8*, 1273, DOI: 10.1038/s41467-017-01249-1

19) Tabandeh, S.; Leon, L. Engineering peptide-based polyelectrolyte complexes with increased hydrophobicity. *Molecules* **2019**, *24*, 868, DOI: 10.3390/molecules24050868

20) Abbas, M.; Lipiński, W. P.; Nakashima, K. K.; Huck, W. T. S.; Spruijt, E. A short peptide synthon for liquid-liquid phase separation. 2020-08-28. ChemRxiv (Organic Chemistry). DOI: 10.26434/chemrxiv.12881288.v1 (Accessed 2021-10-05).

21) Koga, S.; Williams, D. S.; Perriman, A. W.; Mann, S. Peptide-nucleotide microdroplets as a step towards a membrane-free protocell model. *Nat. Chem.* **2011**, *3*, 720–724.

22) Priftis, D.; Tirrell, M. V. Phase behaviour and complex coacervation of aqueous polypeptide solutions. *Soft Matter* **2012**, *8*, 9396-9405.

23) Vieregg, J. R.; Lueckheide, M.; Marciel, A. B.; Leon, L.; Bologna, A. J.; Rivera, J. R.; Tirrell, M. V. Oligonucleotide–peptide complexes: phase control by hybridization. *J. Amer. Chem. Soc.* **2018**, *140*, 1632-1638.

24) Rumyantsev, A. M.; Jackson, N. E.; Yu, B.; Ting, J. M.; Chen, W.; Tirrell, M. V.; de Pablo, J. J. Controlling complex coacervation via random polyelectrolyte sequences. *ACS Macro Lett.* **2019**, *8*, 1296-1302.

25) Nakashima, K. K.; Baaij, J. F.; Spruijt, E. Reversible generation of coacervate droplets in an enzymatic network. *Soft Matter* **2018**, *14*, 361-367.

26) Fraccia, T. P.; Jia, T. Z. Liquid crystal coacervates composed of short double-stranded DNA and cationic peptides. *ACS Nano* **2020**, *14*, 15071-15082.

27) Lu, T.; Nakashima, K. K.; Spruijt, E. Temperature-responsive peptide-nucleotide coacervates. *J. Phys. Chem. B* **2021**, *125*, 3080-3091.

28) Priftis, D.; Leon, L.; Song, Z.; Perry S. L.; Margossian, K. O.; Tropnikova, A.; Cheng, J.; Tirrell, M. Self-assembly of α-helical polypeptides driven by complex coacervation. *Angew. Chem. Int. Ed.* **2015**, *54*, 11128 –11132.

29) Rodriguez, A. R.; Kramer, J. R.; Deming, T. J. Enzyme-triggered cargo release from methionine sulfoxide containing copolypeptide vesicles. *Biomacromolecules* **2013**, *14*, 3610-3614.

30) Kramer, J. R.; Deming, T. J. Multimodal switching of conformation and solubility in homocysteine derived polypeptides. *J. Amer. Chem. Soc.* **2014**, *136*, 5547–5550.

31) Gharakhanian, E. G.; Deming, T. J. Chemoselective synthesis of functional homocysteine residues in polypeptides and peptides. *Chem. Commun.* **2016**, *52*, 5336-5339.

32) Uversky, V. N.; Kuznetsova, I. M.; Turoverov, K. K.; Zaslavsky, B. Intrinsically disordered proteins as crucial constituents of cellular aqueous two phase systems and coacervates. *FEBS Lett.* **2015**, *589*, 15–22.

33) Gharakhanian, E. G.; Deming, T. J. Versatile synthesis of stable, functional polypeptides via reaction with epoxides. *Biomacromolecules* **2015**, *16*, 1802-1806.

34) Chambers, R. W.; Carpenter, F. H. On the preparation and properties of some amino acid amides. *J. Amer. Chem. Soc.* **1955**, *77*, 1522-1526.

35) Wollenberg, A. L.; Perlin, P.; Deming, T. J. Versatile N-methylaminooxy functionalized polypeptides for preparation of neoglycoconjugates. *Biomacromolecules*, **2019**, *20*, 1756-1764.

36) Appel, P.; Yang, J. T. Helix-coil transition of poly-L-glutamic acid and poly-L-lysine in D_2O. *Biochemistry,* **1965**, *4*, 1244-1249.

37) Morrow, J. A.; Segal, M. L.; Lund-Katz, S.; Philips, M. C.; Knapp, M.; Rupp, B.; Weisgraber, K. H. Differences in stability among the human apolipoprotein E isoforms determined by the amino-terminal domain. *Biochemistry* **2000**, *39*, 11657-11666.

38) Deming, T. J. Functional modification of thioether groups in peptides, polypeptides, and proteins. *Bioconjugate Chem.* **2017**, *28*, 691−700.

39) Lu, H.; Wang, J.; Bai, Y.; Lang, J. W.; Liu, S.; Lin, Y.; Cheng, J. Ionic polypeptides with unusual helical stability. *Nat. Commun.* **2011**, *2*, 206–214.

40) Jochum, F. D.; Theato, P. Temperature- and light-responsive smart polymer materials. *Chem. Soc. Rev.* **2013**, *42*, 7468-7483.

41) Wimley, W. C.; Creamer, T. P.; White, S. H. Solvation energies of amino acid side chains and backbone in a family of host-guest pentapeptides. *Biochemistry* **1996**, *35*, 5109-5124.

42) Plamper, F. A.; Ruppel, M.; Schmalz, A.; Borisov, O.; Ballauff, M.; Müller, A. H. E. Tuning the thermoresponsive properties of weak polyelectrolytes: aqueous solutions of star-shaped and linear poly(N,N-dimethylaminoethyl methacrylate). *Macromolecules* **2007**, *40,* 8361-8366.

43) Brot, N.; Weissbach, L.; Werth, J.; Weissbach, H. Enzymatic reduction of protein-bound methionine sulfoxide. *Proc. Natl. Acad. Sci. USA* **1981**, *78*, 2155-2158.

44) Levine, R. L.; Mosoni, L.; Berlett, B. S.; Stadtman, E. R. Methionine residues as endogenous antioxidants in proteins. *Proc. Natl. Acad. Sci. USA* **1996**, *93*, 15036-15040.

45) Levine, R. L.; Moskovitz, J.; Stadtman, E. R. Oxidation of methionine in proteins: roles in antioxidant defense and cellular regulation. *Life* **2000**, *50*, 301-307.

46) Moskovitz, J.; Bar-Noy, S.; Williams, W. M.; Requena, J.; Berlett, B. S.; Stadtman, E. R. Methionine sulfoxide reductase (MsrA) is a regulator of antioxidant defense and lifespan in mammals. *Proc. Natl. Acad. Sci. USA* **2001**, *98*, 12920-12925.

47) Gharakhanian, E. G.; Bahrun, E.; Deming, T. J. Influence of sulfoxide group placement on polypeptide conformational stability. *J. Amer. Chem. Soc.,* **2019**, *141*, 14530-14533.

TOC Graphic:

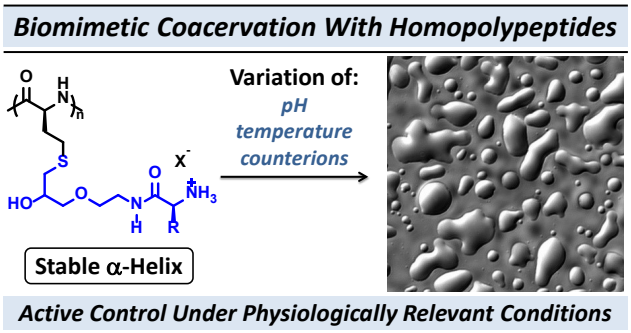
Biomimetic Coacervation With Homopolypeptides
Variation of:
pH
temperature
counterions
Stable α-Helix
Active Control Under Physiologically Relevant Conditions